Electronic Supplementary Material (ESI) for Physical Chemistry Chemical Physics.

Supporting Information

Photoelectrocatalytic degradation of rhodamine B on TiO_2 photonic crystal

Xiuzhen Zheng, Danzhen Li, Xiaofang Li, Linhui Yu, Peng Wang, Xiaoyun Zhang, Jialin Fang, Yu Shao, and Yi Zheng*

Research Institute of Photocatalysis, State Key Laboratory of Photocatalysis on Energy and Environment, Fuzhou University, Fuzhou 350002, P. R. China

Corresponding author Tel & Fax: (+86)591-83779256, E-mail: dzli@fzu.edu.cn.

Summary: **This file contains 20 pages, 17 figures, and 1 table.**

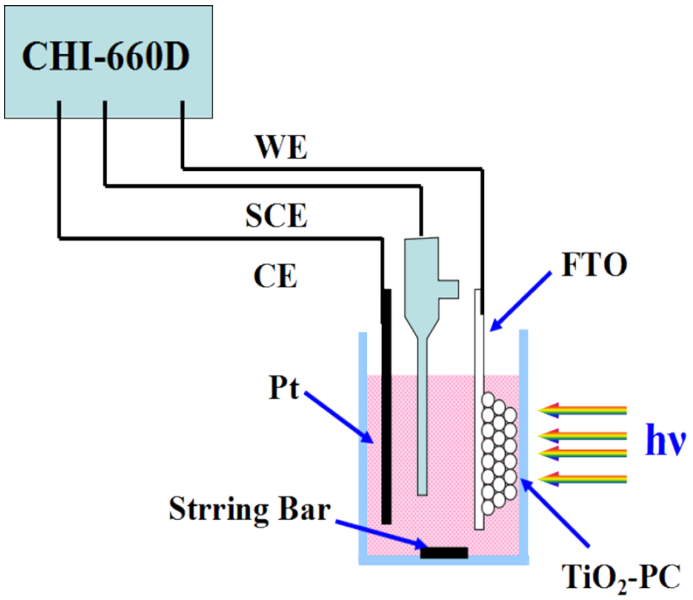

Fig. S1 Schematic diagram showing the PEC degradation process of TiO_2-PCs (WE: working electrode; SCE: saturated calomel electrode; CE: counter electrode).

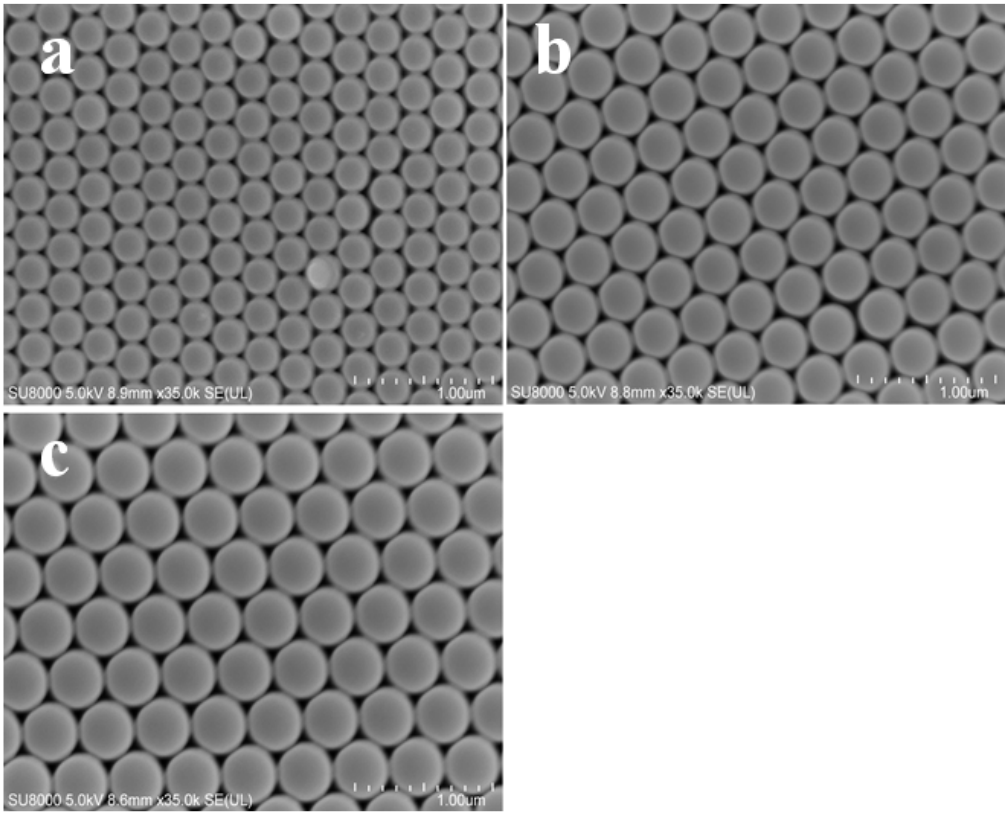

Fig. S2 FESEM image of the PS opal templates with the diameter of 270, 340 and 400 nm.

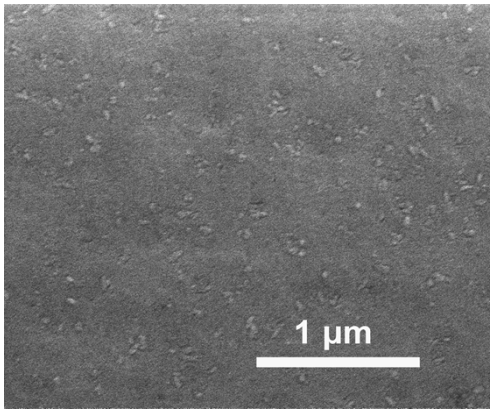

Fig. S3 The SEM image of TiO_2 film.

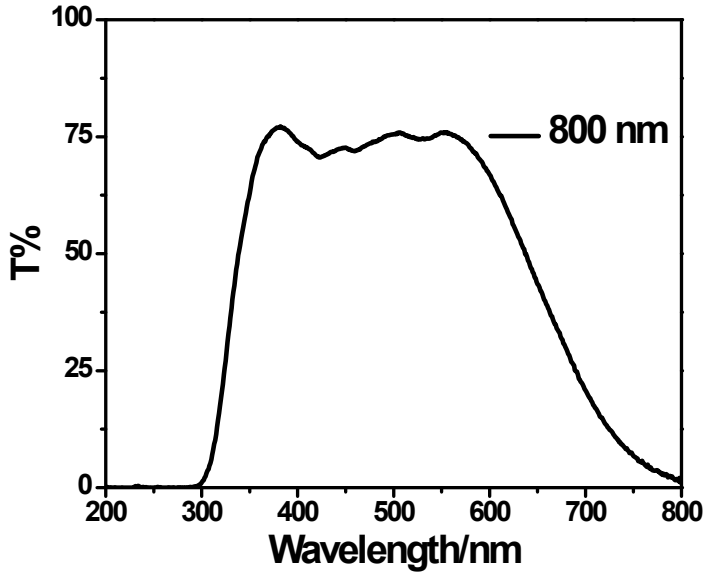

Fig. S4 Transmission spectra of 800 nm cutoff filter.

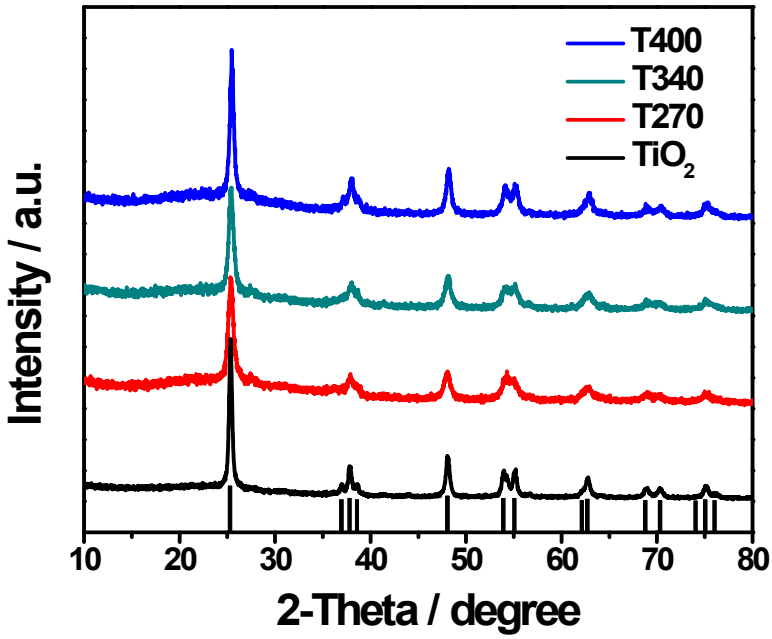

Fig. S5 XRD patterns of TiO_2-PCs and TiO_2 nanoparticles.

Notes:

In the XRD spectra of TiO_2-PCs TiO_2 and TiO_2-PCs (Fig. S5), the characteristic diffraction peaks at 2θ values of 25.3, 37.9, 48.1, 54.0, 55.2, 62.8 can be assigned as (101), (004), (200), (105), (211) and (204) faces of anatase TiO_2, respectively (JCPDS card No. 21-1272). Obviously, TiO_2-PCs and TiO_2 had similar XRD patterns, illuminating that the presence of three-dimensional periodic structure did not have impact on the TiO_2 crystalline phase.

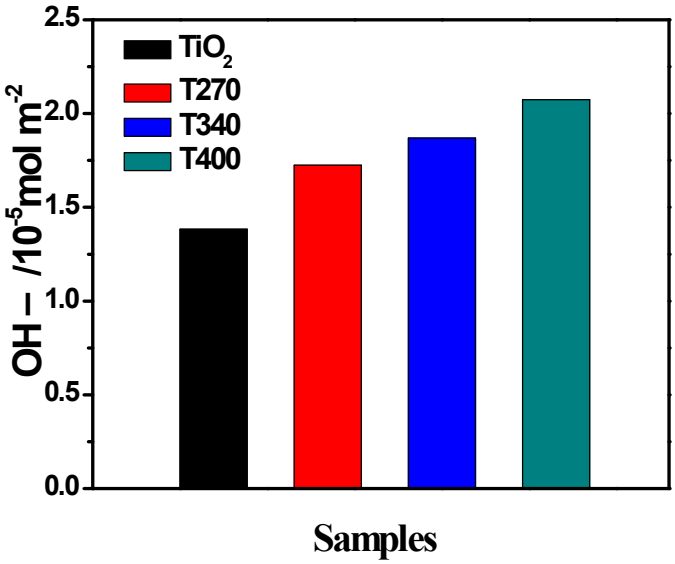

Fig. S6 The amount of OH(a) groups measured with 0.3 mM NaOH.

Notes:

The source of •OH radical are mainly from two ways: one is the reaction between holes and surface hydroxyl groups ($h_{vb}^+ + H_2O\ (OH^-) \rightarrow \bullet OH + H^+$), and the other one is the adsorbed H_2O_2 ($e + H_2O_2 + H^+ \rightarrow \bullet OH + H_2O$).

A special crystal face of TiO_2 bears equal quantities of two types of OH groups: a bridging OH group (surface acidic hydroxyl (OH(a))) bound to a surface Ti^{4+} ion which is four coordinates with respect to the lattice and a terminal OH group (surface basic hydroxyl (OH(b))) bound to a Ti^{4+} ion which is five coordinates with respect to lattice oxide ions.[1, 2] Because the quantities of the two types of hydroxide groups are equal, the total density of OH groups on TiO_2 is twice as much as that of OH(a) groups.[2, 3]

The amount of OH groups on TiO_2 was measured by the method of surface acid–base, ion–exchange reactions for saturation with low concentrations of NaOH.[4] The NaOH concentration of the retrieved solutions decreased due to the reaction with OH(a) groups according to Scheme 2. Detailed experimental procedure could be found in the reference.[5]

Scheme S1. The reaction between NaOH and acidic hydroxyl groups

$$–OH(a) + Na^+ + OH^- \rightarrow –O^- \bullet Na^+ + H_2O.$$

As shown in the Fig. S6, the OH(a) groups of TiO_2-PCs were much higher than that of TiO_2 nanoparticles. In the same way, the total density of OH groups on TiO_2-PCs increased, following the order T400 > T340 > T270 > TiO_2.

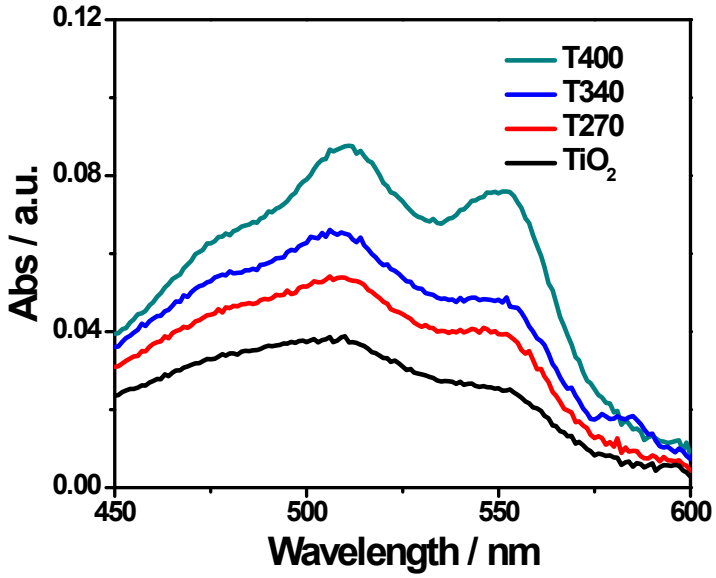

Fig. S7 Absorption spectra of the DPD/POD reagent after reaction with different samples under 30 min of simulated solar light irradiation.

Secondly, the •OH radical can also be generated when H_2O_2 molecule capture a trapped electron.[6] The N,N-diethyl-p-phenylenediamine (DPD) method is widely employed for the detection of H_2O_2. The result was shown in Fig. S7. Apparently, the amount of H_2O_2 followed the order T400 > T340 > T270 > TiO_2, which was in accord with the order of their valence band potential.

Table S1. The kinetic constants (k) of TiO_2-PCs for PEC and photocatalytic degradation under simulated solar light irradiation.

samples	photocatalysis		PEC		Multiples
	k	R^2	k	R^2	
TiO_2	0.0016	0.9913	0.0052	0.9946	3.25
T270	0.0026	0.9941	0.0096	0.9981	3.80
T340	0.0039	0.9969	0.0160	0.9883	4.10
T400	0.0032	0.9981	0.0125	0.9876	3.91

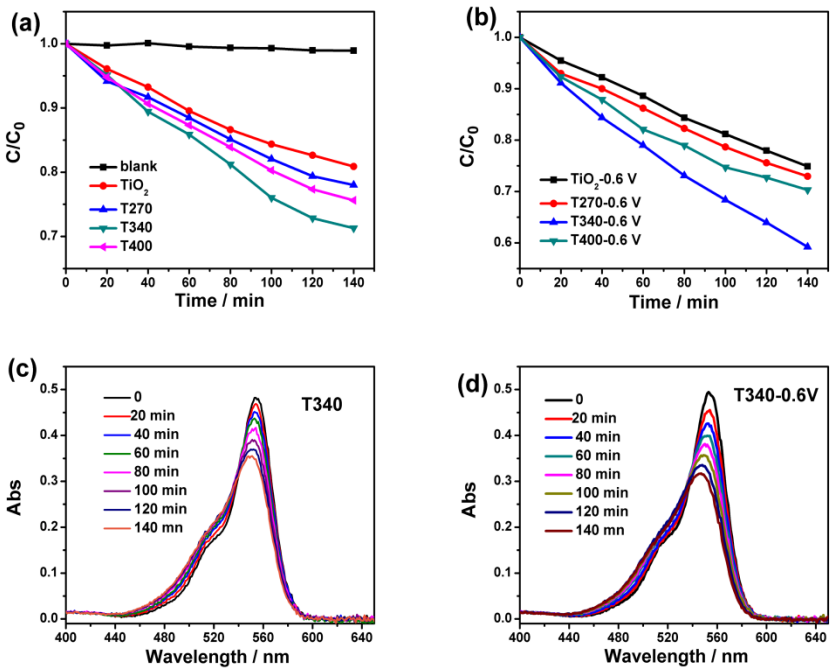

Fig. S8 the liquid-phase photocatalytic (a) and PEC (b) degradation of RhB for TiO_2 films, (c) and (d) were the RhB degradation of T340 and T340-0.6V under visible light irradiation (420 nm < λ < 800 nm).

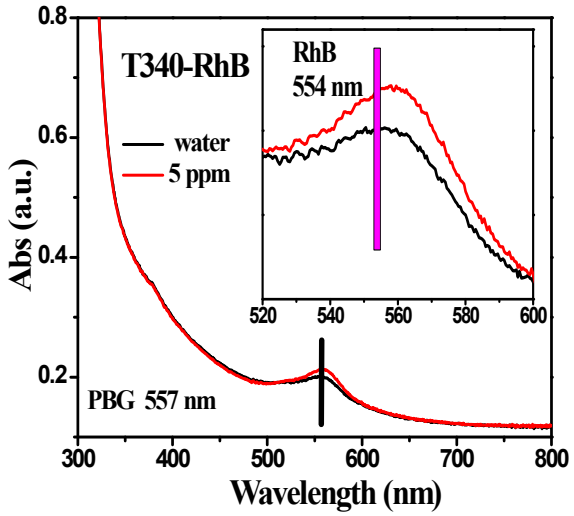

Fig. S9 The absorption spectra of T340 in water and RhB solution.

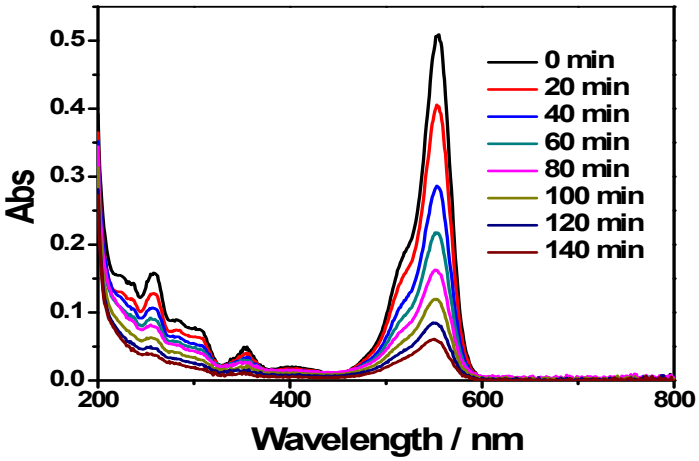

Fig. S10 Liquid-phase degradation of the RhB over T340-0.6V photocatalyst under simulated solar light irradiation (320 nm < λ < 800 nm)

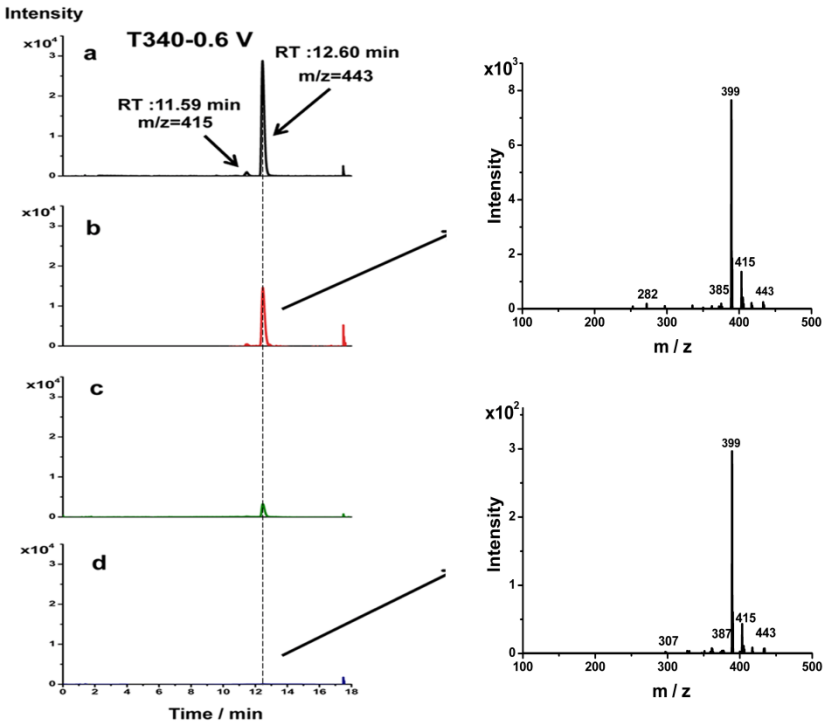

Fig. S11. LC-MS chromatograms of the RhB solution at different irradiation intervals in PEC process: (a) chromatogram of the original RhB solution after adsorption–desorption equilibrium without light irradiation; (b)–(d) chromatogram of RhB solution after 40, 100, and 140min of simulated solar light irradiation, respectively.

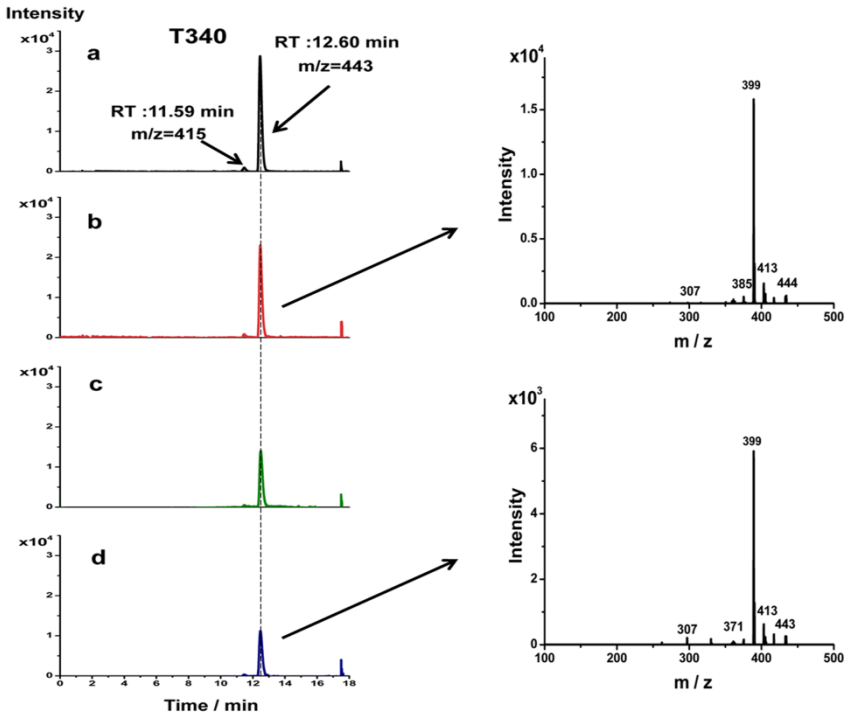

Fig. S12 LC-MS chromatograms of the RhB solution at different irradiation intervals in photocatalytic process: (a) chromatogram of the original RhB solution after adsorption–desorption equilibrium without light irradiation; (b)–(d) chromatogram of RhB solution after 40, 100, and 140 min of simulated solar light irradiation, respectively.

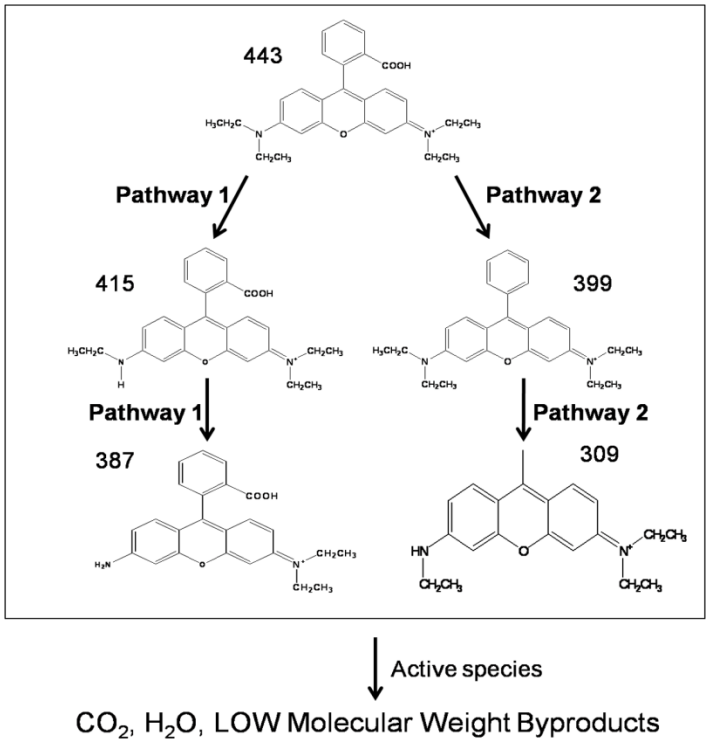

Fig.S13 Proposed degradation pathway of RhB in PEC and photocatalytic process on T340.

Note:

Analysis of the reaction intermediates and final products are useful for evaluating the efficiency of catalytic systems and may reveal some details of the reaction process. Degradation intermediates of RhB in PEC and photocatalytic were identified by LC/MS and GC/MS. Corresponding to the LC/MS identification (Fig. S11 and S12), it was well-known that the RhB degradation occured via two competitive processes. One was stepwise N-de-ethylation (pathway 1), and the other was the destruction of the conjugated structure (pathway 2). In the photocatalysis and PEC process, the main pathway of RhB degradation was the destruction of the conjugated structure (Fig. S13). In PEC system, only a little portion of N, N-diethyl-N'-ethyl-rhodamine could be identified.

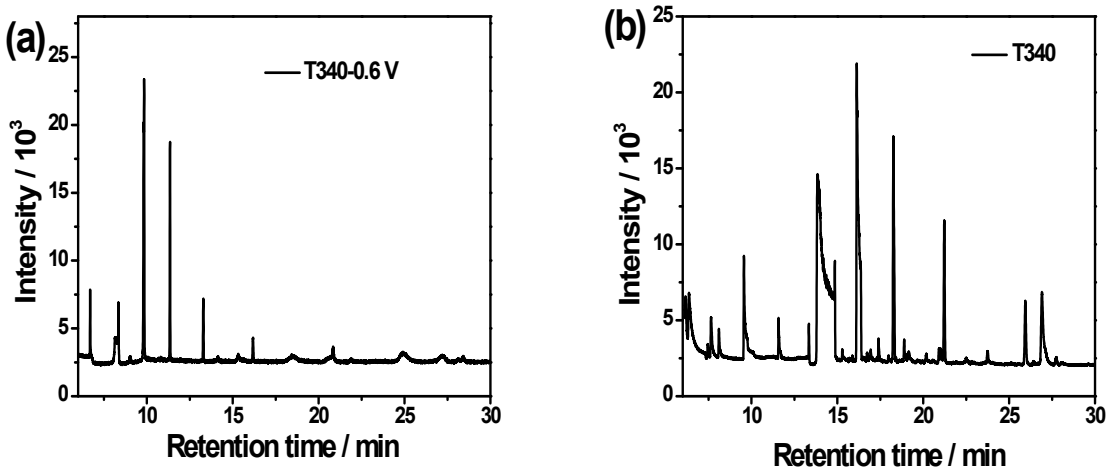

Fig. S14 GC chromatogram of the intermediates obtained from the PEC (a) and photocatalytic (b) degradation of RhB on T340 film.

Note:

As shown in Fig. S14, the retention times of GC for RhB degradation products were different in the photocatalysis and PEC process. The final products detected in the PEC process were less than those in the photocatalytic degradation on T340. This result indicated that the T340-0.6 V exhibited higher degradation efficiency with less organic intermediates.

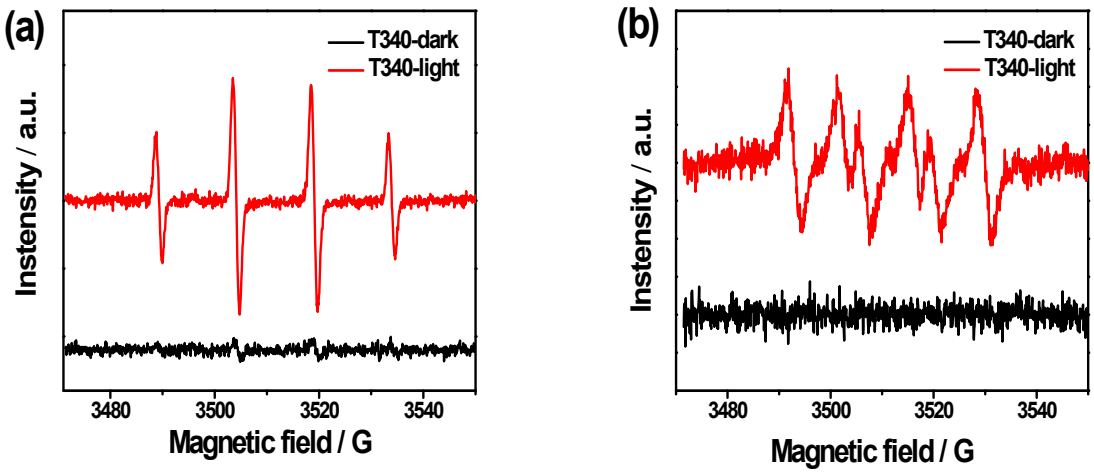

Fig. S15 DMPO spin-trapping ESR spectra of T340 for DMPO-OH• (a) and DMPO-O_2•$^-$ (b) under simulated solar light irradiation.

Notes:

The presence of inverse-opal structure in the T340 was beneficial for the separation of electron/hole pairs, which may cause more radical species with strong oxidation capability, such as hydroxyl radical (•OH) and superoxide radical (O_2•$^-$) species. In order to further confirm that, ESR spin-trapping technique with 5, 5-Dimethyl-1-pyrroline-N-oxide (DMPO) was carried out to detect the active species under simulated solar light irradiation. Fig. S15a showed the ESR spectra of the catalysts/DMPO aqueous dispersions under ambient conditions. As for the T340 sample, a set of signals with four characteristic peaks appeared with the intensity ratio of 1:2:2:1, which are assigned to DMPO-•OH spin adducts. In addition, under simulated solar light irradiation, the six characteristic peaks, corresponding to the spin-adducts DMPO–O_2•$^-$, could be observed in the methanol solvent (Fig. S15b). On the basis of the above analysis, the active species such as O_2•$^-$ and •OH were participated in the degradation process.

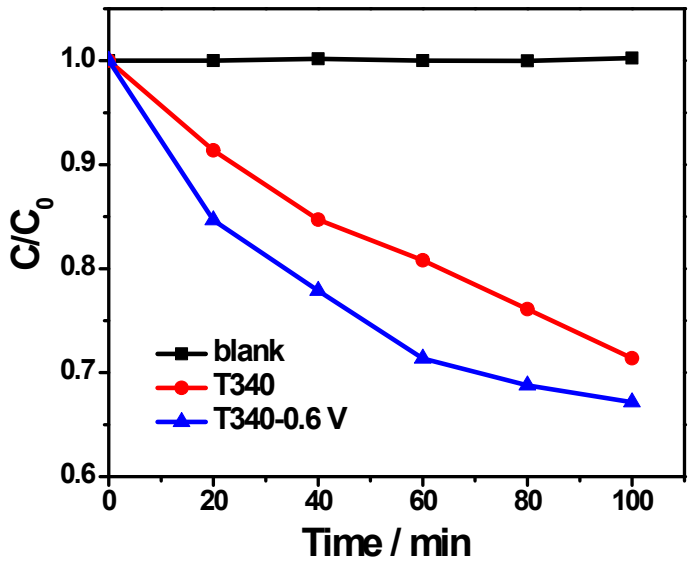

Fig. S16 The variation in the concentration of NBT with T340-0.6 V and T340 samples under simulated solar light irradiation.

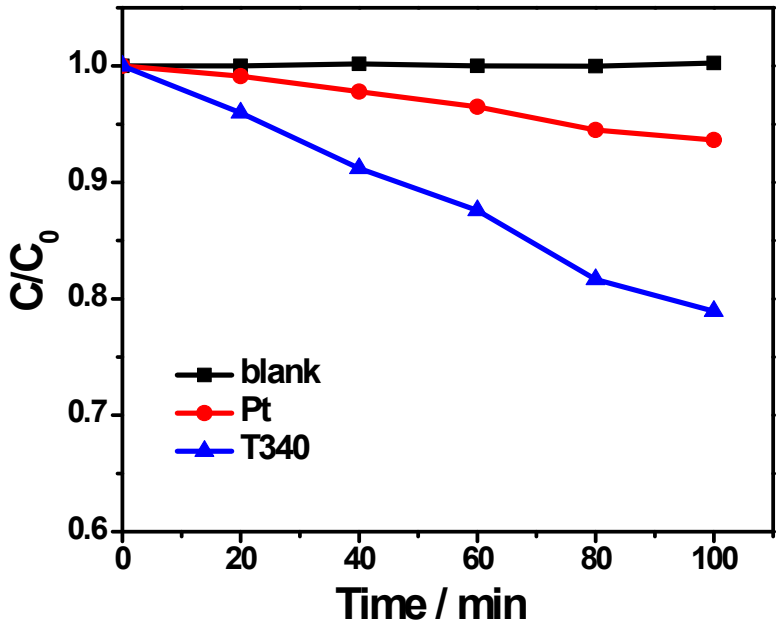

Fig. S17 The variation in the concentration of NBT in the Pt electrode of T340 with 0.6 V under simulated solar light irradiation.

Notes:

The cathode (Pt electrode) and the anode (T340 film) was separated and connected through the salt bridge, with Pt electrode without light irradiation and T340 film under light irradiation. The decrease of NBT concentration in the Pt electrode was used to determine the existent of $O_2^{\bullet -}$ (Fig. S17). It could be deduced that the amount of $O_2^{\bullet -}$ was partial generated in the Pt electrode, and the other part was from T340 electrode. Therefore, the sources of $O_2^{\bullet -}$ in the RhB degradation were twofold at least: (1) the injected electron reacted with the O_2 adsorbed on the surface of Pt electrode, and (2) the departed photoinduced electrons reacted with the O_2 adsorbed on the surface of TiO_2-PC electrode.

References:

1. W. Li, D. Li, Y. Lin, P. Wang, W. Chen, X. Fu and Y. Shao, *J. Phys. Chem. C*, 2012, **116**, 3552-3560.
2. H. P. Boehm, *Discuss. Faraday Soc.* 1971, **52***,* 264−275.
3. H. Tamura, N. Katayama and R. Furuichi, *Environ*. *Sci*. *Technol*., 1996, **30**, 1198-1204.
4. H. Tamura, A. Tanaka, K.-y. Mita and R. Furuichi, *J. Colloid Interface sci.*, 1999, **209**, 225-231.
5. X. Zheng, S. Meng, J. Chen, J. Wang, J. Xian, Y. Shao, X. Fu and D. Li, *J. Phys. Chem. C*, 2013, **117**, 21263-21273.
6. T. Hirakawa and Y. Nosaka, *Langmuir*, 2002, **18**, 3247-3254.